Talanta 116 (2013) 541–547

Contents lists available at ScienceDirect

Talanta

journal homepage: www.elsevier.com/locate/talanta

Calculation of cooperativity and equilibrium constants of ligands binding to G-quadruplex DNA in solution

A.G. Kudrev *

Department of Chemistry, St. Petersburg State University, Russian Federation

ARTICLE INFO

Article history:
Received 11 March 2013
Received in revised form
3 July 2013
Accepted 5 July 2013
Available online 11 July 2013

Keywords:
Cooperativity
Hard modeling
G-quadruplex
TMPyP4

ABSTRACT

Equilibrium model of a ligand binding with DNA oligomer has been considered as a process of small molecule adsorption onto a lattice of multiple binding sites. An experimental example has been used to verify the assertion that during saturation of the macromolecule by a ligand should expect effect of cooperativity due to changes in DNA conformation or the mutual influence between bound ligands. Such phenomenon cannot be entirely described by the classical stepwise complex formation model. To evaluate a ligand binding affinity and cooperativity of ligand–oligomer complex formation the statistical approach has been proposed. This new computational approach used to re-examine previously studded ligand binding towards DNA quadruplexes targets with multiple binding sites. The intrinsic equilibrium constants $\boldsymbol{K}_{1-3}$ of the mesotetrakis-(N-methyl-4-pyridyl)-porphyrin (TMPyP4) binding with the $[d(T_4G_4)]_4$ and with the $[AG_3(T_2AG_3)_3]$ quadruplexes and the correction for the mutual influence between bound ligands (cooperativity parameters ω) was determined from the Job plots based upon the nonlinear least-squares fitting procedure. The re-examination of experimental curves reveals that the equilibrium is affected by the positive cooperative ($\omega > 1$) binding of the TMPyP4 ligand with tetramolecular $[d(T_4G_4)]_4$. However for an intramolecular antiparallel–parallel hybrid structure $[AG_3(T_2AG_3)_3]$ the weak anti-cooperativity of TMPyP4 accommodation ($\omega < 1$) onto two from three non-identical sites was detected.

1. Introduction

During the recent years, numerous investigations have been devoted to the study of small molecules binding with four-stranded DNA structures known as G-quadruplexes (G4) for the discovery of new anti-cancer agents and developing tools for elucidating the role of those structures [1,2]. The G4 structures appealing targets for drug development because of the molecules–ligands that interact strongly with quadruplex DNA are able to inhibit telomerase [3]. Hence, there is a great current interest in developing ligands that interact with quadruplexes. To fully exploit this challenging approach, however, we need to better understand the mechanism of G-quadruplexes interactions with ligands, specificity of a ligand (duplex vs. quadruplex) and binding mode of a ligand.

In the present study the binding of the cationic mesotetrakis-(N-methyl-4-pyridyl)-porphyrin (TMPyP4) to G-quadruplexes (see Schemes 1 and 3) was selected as experimental example for the validation of the proposed hard modeling of a ligand interaction with the DNA oligomer.

Several studies were shown that TMPyP4 stabilize different types of G4 structures [4–6]. This porphyrin have considered as a promising quadruplex stabilising molecule with potential applications as anti-tumor therapeutic agent since it can induce telomerase inhibition upon binding to telomeric DNA quadruplexes [7]. The selectivity of TMPyP4 for the quadruplex relative to duplex DNA investigations [4] reinforces the potential applications of TMPyP4 [8]. The recent studies revealed that TMPyP4 cationic porphyrin can induce the formation of a DNA quadruplex from a single-stranded oligonucleotide [9].

The TMPyP4 molecule has been extensively used as a probe of G-quadruplexes structure [10]. But, the binding mode (groove binding or binding to loops or intercalation or end-stacking mode) of the TMPyP4 to G-quadruplex, particularly for G-quadruplexes structures from human telomeric sequences, to date still is a point of debate in the literature [11]. In the earliest works, based on the results of ITC and molecular dynamics simulation was proposed the intercalation mode in a parallel G-quadruplex structure [12]. But later by the molecular dynamics calculations were shown that the favored mode of TMPyP4 binding is external stacking rather than the intercalative model. The end-stacking mode in which TMPyP4 binds to quadruplex DNA primarily by stacking with the outer layer of the guanine tetrad has been proposed [13]. Both the end-stacking and the intercalation modes of binding to anti-parallel G4 was accepted in [14]. The groove binding mode has been proved by the crystallography result [15]. This crystal structure investigation shows a loop stacking mode in a TMPyP4-G4 complex formed by parallel $[d(TAG_3T_2AG_3)]$ sequence. Evidence for intercalation was shown for binding of TMPyP4 to the

* Tel.: +7 91 12 998492.
E-mail address: kudrevandrei@mail.ru

0039-9140/$ - see front matter © 2013 Elsevier B.V. All rights reserved.
http://dx.doi.org/10.1016/j.talanta.2013.07.012

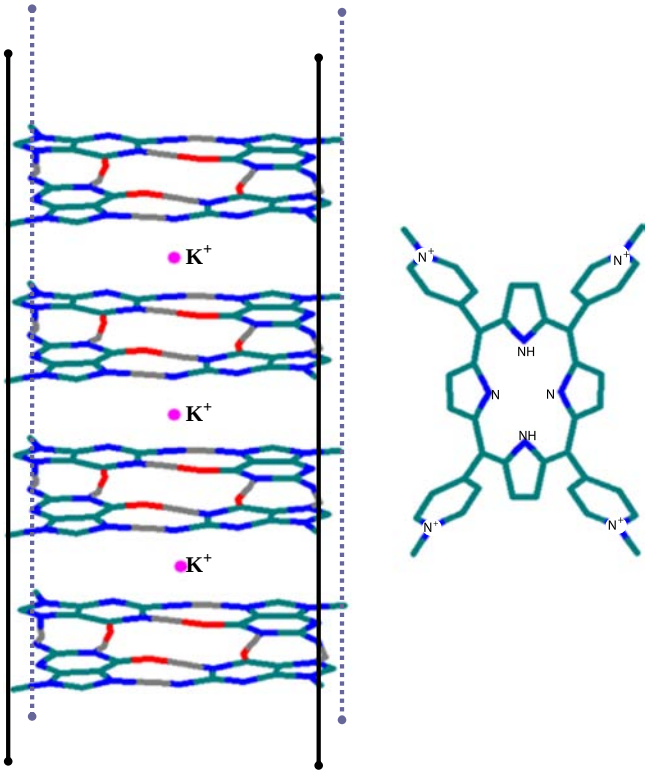

Scheme 1. Schematically shown molecular structure of tetramolecular $[d(T_4G_4)]_4$ quadruplex and cationic porphyrin TMPyP4.

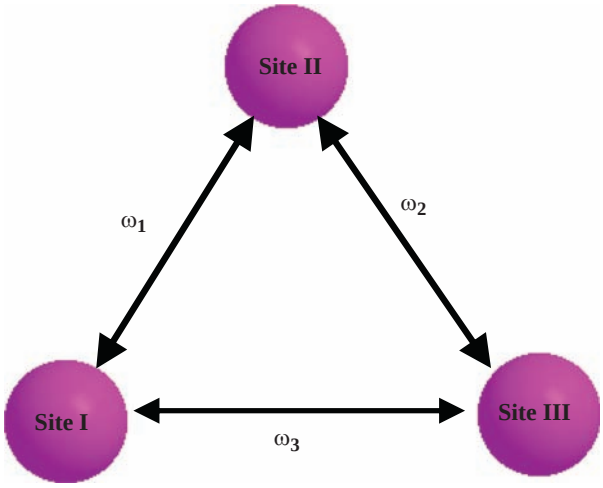

Scheme 2. Postulated mutual influence between sites in the studied systems. Here ω_i is coefficient of cooperativity.

K-free form of the G-quadruplex wires, but the presence of K^+ in the space between the guanine planes hence prevents intercalation into G-quadruplexes [16]. The end-stacking to the external G-tetrads and electrostatic binding to the bases of the larger loops were shown in [17,18]. Time-resolved fluorescence anisotropy study on the interaction between TMPyP4 and four distinct G-quadruplex DNAs, that is, $[AG_3(T_2AG_3)_3]$, thrombin-binding aptamer, $[(G_4T_4G_4)_2]$, and $[(TG_4T)_4]$ revealed a new sandwich-type binding mode in which both terminal G-quartet and (TT) base pair stack on the porphyrin ring through π–π interaction [19].

The binding mode is critically important for understanding the binding stoichiometry which is one of the most important hard modeling parameters. On the other hand we can more precisely predict binding mode if the stoichiometry and intrinsic binding constants will be determined from experimental data. Perhaps this is the key to understanding the mechanism of the G-quadruplex stabilization due to TMPyP4 binding. Several examples reported previously [9,12,14,20–22] parameters of TMPyP4 binding to G-quadruplexes summarized in Table 1 illustrate that the stoichiometries of complexes TMPyP4 with G4 varies depending on DNA sequence forming G4 and on experimental conditions (pH, the presence of K^+ or Na^+ etc.). In details the influence of pH on the TMPyP4 binding with G4 has been studied in [23,24].

To simulate quadruplex–ligand interactions the model based upon a multiple set of independent binding sites has been proposed [25,26]. But this method does not take into account the cooperativity (mutual influence) in the course of successive ligand binding. The thermodynamic effect of cooperativity may be due to changes in the DNA conformation or redistribution the electron density at the site due to the influence through oligomers bonds or by the mutual influence between bound ligands. However, to date, in studies of binding of metal complex and other ligands with G4-quadruplexes parameters of cooperativity were not calculated or discussed [27,28].

Theory of cooperative ligand binding is well known [29]. A number of mathematical models have been developed for such interactions [30–35]. To describe the interactions small molecules with

Table 1
Some previously reported stoichiometries (n) and equilibrium constants ($\lg K_b$, M^{-1}) of TMPyP4 porphyrin binding to G-quadruplexes DNA.

G4 tetraplex	n	$\lg K_b$	Method	Remarks	Ref.
$[d(G_2T_2G_2TGTG_2T_2G_2)]$	$n_1=1$	5.25	ITC	pH 7, 25 °C, K^+–BPES	[12]
$[d(G_2T_2G_2TGTG_2T_2G_2)]$	$n_1=1.2$	5.34	SP	pH 7, 25 °C, K^+–BPES	[12]
$[d(T_4G_4)]_4$	$n_1=2.9$	4.89	ITC	pH 7, 25 °C, K^+–BPES	[12]
$[d(T_4G_4)]_4$	$n_1=2.6$	5.23	SP	pH 7, 25 °C, K^+–BPES	[12]
$[d(T_4G_4)]_4$	$n_1=0.9$	6.63	SP	pH 7, 25 °C, Na^+–BPES	[12]
$[d(AG_3(T_2AG_3)_3)]$	$n_1=1.9$	4.45	ITC	pH 7, 25 °C, K^+–BPES	[12]
$[d(AG_3(T_2AG_3)_3)]$	$n_1=1.8$	4.87	SP	pH 7, 25 °C, K^+–BPES	[12]
$[d(AG_3(T_2AG_3)_3)]$	$n_1=1.55$ $n_2=1.2$	6.03 8.65	SP	pH 7.5, 150 mM K^+	[20]
$[d(AG_3(T_2AG_3)_3)]$	$n_1=1.48$ $n_2=0.54$	6.94 8.35	SP	pH 7.5, 150 mM K^+, 40% PEG	[20]
$[d(AG_3(T_2AG_3)_3)]$	$n_1=4$	–	SP	pH 7.5, Tris–HCl; 100 mM Na^+	[14]
$[d(TAG_3(T_2AG_3)_3T)]$	$n_1=6.1$ ($n_1\approx5$)	6.81	SP; (CD; FL)	pH 7.2, 25 °C, Tris–HCl	[9]
$[d(TAG_3(T_2AG_3)_3T)]$	$n_1=4.6$ ($n_1\approx4.9$)	6.80	SP; (CD; FL)	pH 7.2, 25 °C, Tris–HCl, 10 mM K^+	[9]
$[d(TAG_3(T_2AG_3)_3T)]$	$n_1=2.7$ ($n_1\approx2.8$)	6.25	SP; (CD; FL)	pH 7.2, 25 °C, Tris–HCl, 100 mM K^+	[9]
$[d(G_3(T_2AG_3)_3)]$	$n_1=1.1$ $n_2=1.7$	6.70 6.04	SP	pH 7.0, 25 °C, 100 mM K^+	[21]
$[d(G_3(T_2AG_3)_3)]$	$n_1=1$ $n_2=2$	6.60 5.70	ITC	pH 7.0, 25 °C, 100 mM K^+	[21]
$[d(G_3T)_3G_3]$	$n_1=0.8$ $n_2=1.0$	7.85 6.32	SP	pH 7.0, 25 °C, 100 mM K^+	[22]
$[d(G_3T)_3T_2G_3]$	$n_1=0.7$ $n_2=2.0$	8.20 6.30	SP	pH 7.0, 25 °C, 100 mM K^+	[22]
$[d(G_3T)_3T_4G_3]$	$n_1=1.2$ $n_2=2.2$	8.75 6.40	SP	pH 7.0, 25 °C, 100 mM K^+	[22]

n_1 and n_2 are the phenomenological stoichiometries of TMPyP4-quadruplex interaction; ITC is isothermal titration calorimetry; SP is spectrophotometry; K^+ (Na^+)-BPES is $K(Na)H_2PO_4/K(Na)_2HPO_4$, K(Na)Cl, EDTA buffer; PEG is poly(ethylene glycol); FL is fluorescence.

homogeneous polymers is most commonly used model, which takes into account the mutual influence between the nearest neighboring bound ligands. For this case McGhee and von Hippel was derived convenient statistical equation of adsorption [35]. Now this equation along with the classical Scatchard equation [36] are the most commonly used, and in fact have become standard in the interpretation of ligands with polymers interactions. However, sometimes those equations incorrectly used to describe interactions with G-quadruplexes and other DNA nonhomogeneous oligomers despite the fact that McGhee and von Hippel have concluded, that the binding of ligands known to have heterogeneous binding sites on the DNA cannot be adequately treated based on the conditional probability approach [35]. Also, it was shown that the Scatchard plot and so called Ditect plot are not suitable for evaluating the binding of TMPyP4 to G-quadruplexes [14].

The aim of the present paper is to give general description an equilibrium association of a ligand with heterodentate oligomer (a molecule with multiple nonidentical binding sites), and as example to calculate the equilibrium parameters of TMPyP4 binding to the G-quadruplex target on the base of modified matrix method. This method should provide equilibrium constants and cooperativity parameters for solution equilibrium involving a small molecule and heterodentate DNA oligomer.

2. Computational details

To compute the intrinsic constants of a ligand binding with heterodentate oligomer we analyze experimental data presented in the form of Job plots (continuous variation analysis). In this univariate method the absorbance data recorded to characterize the progress of a reaction monitored at a single wavelength. It is well known that the method correctly identifies stoichiometry only in the case of a single complex formation. But these quantitative data can be used to calculate equilibrium constants. In the experimental work the fraction of bound TMPyP4 was calculated using observed response R which is proportional to the amount of bound drug.

$$F_{exp} = R/\max(R) \tag{1}$$

here $R=(A_f-A)/(A_f-A_b)$, (r.u.); A_f and A_b are the absorbance of the free and fully bound drug, and A is the absorbance at any given point during the titration; r.u. is response units. The max(R) per bound molecule is the theoretical maximum response and is proportional to the amount of immobilized ligand. The max(R) value is required to estimate the standard binding parameters such as moles of drug bound per moles of DNA binding sites. Simulations show that the function $F_{exp}=f(r)$ (here r is the mole fraction of ligand) coincides with the theoretical function $F_{calc}=f(r)$ computed by the equation

$$F_{calc} = (C_L-[L])/\max(C_L-[L]) \tag{2}$$

here $[L]$ and C_L are equilibrium and total concentrations of ligand respectively. To calculate F_{calc} for the system under study it is necessary to modify the standard approach.

In previous papers was proposed to calculate the equilibrium constants which govern the binding of small molecules upon a set of equivalent sites in coordination compound [37–39] and in homogeneous oligomer [40–45] with help of the matrix method. The thermodynamic description of ligands binding to nonhomogeneous oligomer is the same as adsorption of ligands onto homogeneous oligomer which was described previously [40–45]. To modify matrix approach let us introduce one-dimension matrix of site-specific intrinsic equilibrium constants $\boldsymbol{K}_{1-N}$ ($\boldsymbol{K}_{1-N}$ are constants for a ligand binding to each isolated site 1,…, N), and matrix $\boldsymbol{\Omega}$ of mutual influence corrections (cooperativity parameters ω_1, ω_2,…, ω_N). New is that it will be assumed that energy of binding unique for each site and depends on the presence of other bound ligands in the vicinity. A singly contiguous site, for instance, I is the site to which a ligand binds with association constant $K_i\omega_j$. To a double contiguous site a ligand binds with association constant $K_i\omega_j\omega_k$. The cooperativity parameters ω_j, ω_k are amendments of the equilibrium constant K_i which take into account the mutual influence between equivalent ligands incoming in the nearest environment of site I. The matrix $\boldsymbol{\Omega}$ constructed in accordance with the hypothesis about structure of adducts formed in stepwise process of filling oligomer by a ligand. In general case the number of neighbors is limited only by the total number of binding sites ($j=1, 2,\ldots, N-1$). The values of $\boldsymbol{K}_{1-N}$ and ω_i could be found simultaneously in the following way.

Consider the row of complexes $Poly(L)_n$ ($n=1, 2\ldots, N$) which are present in a solution. The summation of simple combinations of n bound ligands among N binding gives the number of possible variants (m_N) of coordination of N ligands to a central molecule having N sites is computed by the equation

$$m_N = \sum_{n=o}^{N} m_s = \sum_{n=0}^{N} \frac{N!}{n!(N-n)!} = 2^N \tag{3}$$

here n and m_s are numbers of coordinated ligands and number of microstates. In accordance with formula (3) 2^N microstates of complexes formed by an oligomer molecule are possible. The matrix of configurations $\boldsymbol{M}$ has been introduced in order to describe the detailed set of configurations adopted by the macromolecule in microstates. Each line of the matrix $\boldsymbol{M}$ displays a microstates configuration through a sequence of zeroes in those positions where the sites of multidentate macromolecule are not occupied by a ligand, and with a sequence of ones in those positions where the sites are bound to the ligand. In the course of the macromolecule sites saturation, previously bound ligands can affect the binding of following ligands. A row by row multiplication of the configurations matrix $\boldsymbol{M}$ and intrinsic constants $\boldsymbol{K}_{1-N}$ and taking into account mutual influence ω_i gives the matrix $\boldsymbol{M}^*$ (see Supplement 1). For instance, for the oligomer containing three nonidentical binding sites the matrix $\boldsymbol{M}^*$ can be written as

$$\boldsymbol{M}^* = \begin{bmatrix} 0 & 0 & 0 \\ K_1 & 0 & 0 \\ 0 & K_2 & 0 \\ 0 & 0 & K_3 \\ K_1\omega_1 & K_2\omega_1 & 0 \\ K_1\omega_3 & 0 & K_3\omega_3 \\ 0 & K_2\omega_2 & K_3\omega_2 \\ K_1\omega_3 & K_2\omega_1\omega_2 & K_3\omega_3 \end{bmatrix} \tag{4}$$

The mutual influence in the system can be illustrated by Scheme 2. The product of the nonzero elements in the matrix $\boldsymbol{M}^*$ rows gives the stability constants of microscopic species $\boldsymbol{B}$.

$$\boldsymbol{B} = \prod_{j=1}^{N} (\boldsymbol{M}^* - \boldsymbol{M} + 1) \tag{5}$$

The estimates of the true nonlinear parameters $\boldsymbol{K}_{1-N}$ and ω_i allows calculating the concentration of bound ligand for the i-th total concentration of ligand and oligomer, correspondingly C_L and C_P. The concentration of bound ligand is expressed as

$$C_L - [\mathbf{L}] = \frac{\mathbf{S}[\mathbf{L}]^s B}{1 + [\mathbf{L}]^s B} C_P \tag{6}$$

here $S = \Sigma_{j=1}^{N} M^T$ is a row of stoichiometric coefficients. After substituting (6) in Eq. (2), using non-linear least square (LS) refinement find $\lg \boldsymbol{K}_{1-N}$ and $\boldsymbol{\omega_i}$. The oligomer microforms equilibrium concentrations $[Poly(L)_s]$ can be calculated from the formula,

$$[\boldsymbol{Poly}(\boldsymbol{L})_s] = \prod_{j=1}^{N} (\boldsymbol{M}^*[L] - \boldsymbol{M} + 1) = [Poly][L]^s B \tag{7}$$

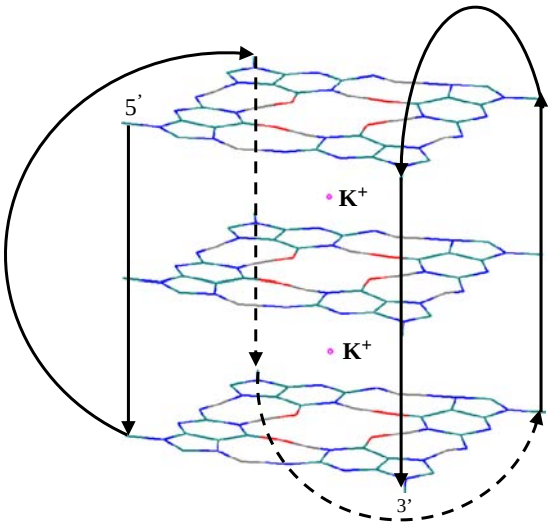

Scheme 3. Schematically shown folding of $[AG_3(T_2AG_3)_3]$ quadruplex intramolecular antiparallel–parallel hybrid structure.

here $[Poly] = C_P/(1 + [L]^S B)$ is an equilibrium concentration of free oligomer. The summation of microforms concentrations gives the concentration of oligomer species corresponding to n bound ligands:

$$C_{formPL}(i) = \left[[Poly] \ldots \sum_{i=1}^{m_s} [Poly(L)_s] \ldots [Poly(L)_N] \right] \quad (8)$$

here m^s is the number of microstates (see Eq. (1)). Eq. (7) allows us to calculate the matrix of species concentrations $\boldsymbol{C}_{formPL}$ for all ligand concentrations in solution. The graph of $\boldsymbol{C}_{formPL}$ is the distribution diagram of oligonucleotide between equilibrium species. Finally using the matrix method it is possible to calculate concentrations of sites (I, II…, N) bound with ligand and amount of bound ligand to each site i.e. $\forall j$ ($j = 1, 2, \ldots, N$):

$$[Mon_jL] = [Poly(L)_s] \cdot \boldsymbol{M} \quad (9)$$

2.1. The procedure of LS fitting

The Levenberg–Marquard LS algorithm [46–48] is used to refine the chemical model parameters $\lg \boldsymbol{K}_{1-N}$ and ω_i from Job diagram. The iterative procedure is used to find the minimum of the objective function:

$$\mathbf{S} = \sum (\mathbf{F_{exp}} - \mathbf{F_{calc}})^2 \quad (10)$$

In this case, the sum of squares of deviations of all F_{exp} were calculated from the corresponding F_{calc} values considered on the current iterative step calculated in turn by using Eq. (2). Theoretical curves are computer generated in accordance with Eq. (2) for trial values of parameters (based upon hypothesis about mutual influence model) until a best fit is obtained. The fitting process minimizes the summed square of the residual $\boldsymbol{S}$. Refinement was stopped when the relative difference in $\boldsymbol{S}$ between consecutive iterations fell below a threshold value. The lack of fit (*lof*) factor [49] was used in the present work to compare matrices by applying the following equation:

$$\mathbf{lof} = \sqrt{\frac{\mathbf{Trace}[(\mathbf{F_{exp}} - \mathbf{F_{calc}})(\mathbf{F_{exp}} - \mathbf{F_{calc}})^{\mathbf{T}}]}{\mathbf{Trace}[\mathbf{F_{exp}} \mathbf{F_{exp}^T}]}} \times 100 \quad (11)$$

here *Trace* is the sum of the diagonal elements. When convergence is achieved data fitting should give *lof* values close to the noise levels.

3. Results and discussion

3.1. The validation of the matrix method

In order to test the capacity of the proposed computational approach, the absorbance data matrix was simulated. The data set was designed to simulate an interaction ligand with oligomer (TMPyP4 with G-quadruplex DNA), which has three independent binding site. For studied systems the mutual influence is depicted in Scheme 2. According to Lambert–Beer's law, a spectrometrically measured absorbance data matrix $\boldsymbol{A}_{sim}$ can be calculated as product of a concentration matrix $\boldsymbol{C}$ and a matrix $\boldsymbol{E}$ of molar absorptivities. The corresponding matrix equation is given as

$$\boldsymbol{A}_{sim} = \boldsymbol{CE} + R \quad (12)$$

The number of rows in matrix $\boldsymbol{A}_{sim}$ is equal to the number of studied solutions with different components concentrations. The number of columns in matrix $\boldsymbol{A}_{sim}$ is equal to the number of wavelengths, and in the current simulations the noise R was put to zero. To build realistic Job plots a variation in the spectra of free TMPyP4 which is usually observed in coordination TMPyP4 to G4 have been simulated (the induced bathochromic red shifts (15–20 nm), and hypochromicities at the λ_{max} (60–70%) of the Soret band). Spectra used to build the data sets simulating the G4–ligand interaction are shown in Supplementary material (Fig. S1). Concentration matrix $\boldsymbol{C}$ can be computed either as a matrix of species concentrations $[\boldsymbol{Poly}(\boldsymbol{L})_s] \cdot \boldsymbol{M}$ or as matrix of the bound site concentrations $[\boldsymbol{Mon_jL}]$. These matrices in accordance with Eq. (9) are identical.

3.2. Simulations of the cooperative ligand binding

Previously the dissociation constant of the complex TMPyP4-$[d(T_4G_4)]_4$ was estimated as 10 μM [12]. According to this pattern for a hypothetical oligomer, comprising three binding sites the following intrinsic constants $\lg \boldsymbol{K}_{1-3} = [5\ 5\ 5]$ are postulated. Fig. 1 shows the Job plots $F_{exp} = f(r)$ (response units, r.u.) calculated from simulated data matrix $\boldsymbol{A}_{sim}$ with help of Eq. (1) at various fixed cooperativity ω_i values. Curvature and the location (abscissa) of the Job plots maximum in dilute solutions, strongly depends on the equilibrium species concentrations and stability. For simulations of the Job plots, the sum of total concentration $C_L + C_P = 5$ μM was kept constant, the same as in the experimental study [12]. However, as seen from the left top part of Fig. 1(1a) under these conditions without cooperativity ($\omega_1 = \omega_2 = \omega_3 = 1$) the function F_{exp} has max at $r = 0.57$, meaning G4:L formal (a phenomenological) stoichiometry is 1:1.3. From species distribution diagram (see Fig. 1a) clear that for all concentrations predominated complex 1:1. The top right as well as bottom parts of Fig. 1 plots F_{exp} with maximum at $r = 0.73$ (formal stoichiometry 1:2.7) which one can observe in the case when the ligand binding is positively cooperative just between sites I–II and II–III i.e. $\omega_1 = \omega_2 = 7$, $\omega_3 = 1$ (see Fig. 1b) or when cooperativity between all three sites is equal among each other i.e. $\omega_1 = \omega_2 = \omega_3 = 3$ (see Fig. 1d). The left bottom part of Fig. 1c shows F_{exp} when cooperativity between only two sites 1 and 3 ($\omega_1 = \omega_2 = 1$, $\omega_3 = 10$) gives maximum at $r = 0.67$ (formal stoichiometry 1:2).

The result of simulations suggests that TMPyP4-$[d(T_4G_4)]_4$ binding constants published in [12] were underestimated, in fact binding constants should be higher, or the alternative explanation is the successive ligand binding governed by positive cooperativity.

3.3. The anti-cooperative ligand binding

Consider a hypothetical oligomer having intrinsic constants $\lg \boldsymbol{K}_{1-3} = \mathbf{[8\ 8\ 8]}$ for sites (I–III) respectively. The anti-cooperativity here simulated in the same way as cooperativity just by substituting of cooperativity parameter for $\boldsymbol{\omega_i} < 1$. For simulations of the anti-cooperativity the sum of concentration $C_L + C_P$ was fixed at 10 μM

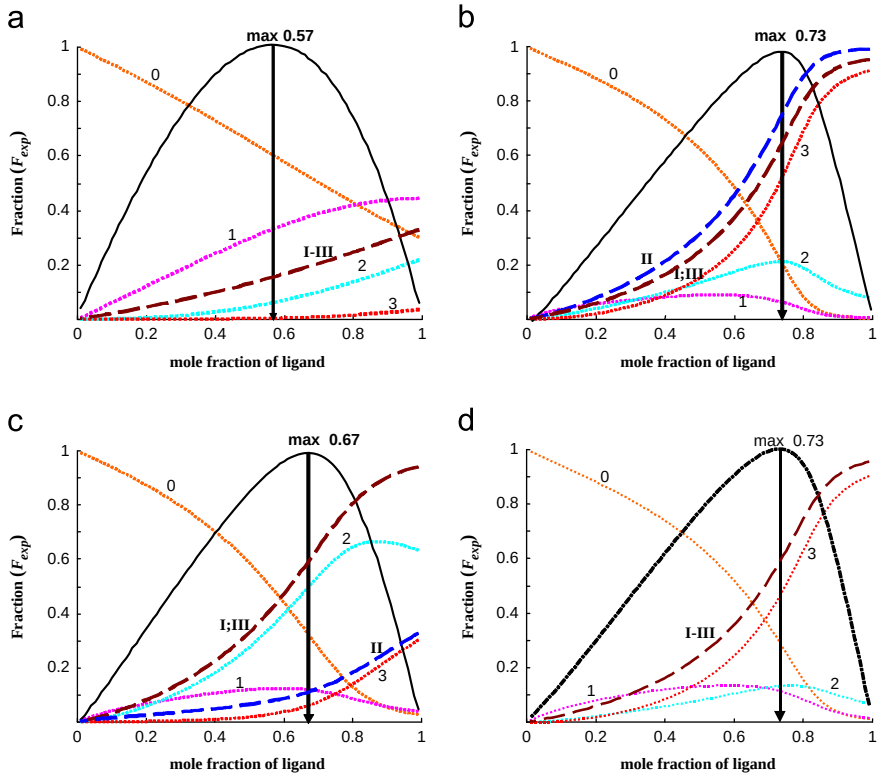

Fig. 1. Simulated Job plots (F_{exp} r.u.) for various ligands toward a oligomer binding positive cooperativity shown as solid lines; (a) $\omega_1=\omega_2=\omega_3=1$; (b) $\omega_1=\omega_2=7$; $\omega_3=1$; (c) $\omega_1=\omega_2=1$; $\omega_3=10$; (d) $\omega_1=\omega_2=\omega_3=3$. The distribution plots of Poly between species $[Poly](L)_n$ as a function of ligand mole fraction (calculated with the help of Eq. 8) shown as dotted lines 0 – not bonded, 1 – 1:1, 2 – 1:2, 3 – 1:3; fractions of sites (I–III) bound with ligand (calculated by Eq. (9)) shown as dashed line; in all cases $\lg \boldsymbol{K}_{1-3}=$**[5 5 5]** and $C_L+C_P=5$ μM.

(the same conditions were used in the experimental study [20]). Fig. 2a shows that under these conditions without cooperativity ($\boldsymbol{\omega}_1=\boldsymbol{\omega}_2=\boldsymbol{\omega}_3=1$) the function F_{exp} has max at $r=0.74$. As expected, formal stoichiometry 1:3 coincides with the true stoichiometry of G4 $(L)_3$ formed when G4 is saturated. For oligomer having lower to ligand affinity the function F_{exp} maximum is shifted to lower values of r. For instance, for oligomer $\lg \boldsymbol{K}_{1-3}=$**[6 8 6]** formal stoichiometry is 1:2.1 (see Fig. 2b). The negatively cooperative ligand binding shifts F_{exp} maximum similar to what is observed at lower binding constants. But worth to note that species distribution is distinctly different. As an example, Fig. 2c shows F_{exp} for oligomer $\lg \boldsymbol{K}_{1-3}=$**[8 8 8]** when anti-cooperativity between only two sites I and III ($\boldsymbol{\omega}_1=\boldsymbol{\omega}_2=1$, $\boldsymbol{\omega}_3=0.10$) gives maximum at $r=0.68$ the same as for oligomer $\lg \boldsymbol{K}_{1-3}=$**[6 8 6]**. The incorporation of gain anti-cooperativity leads to a stretching of species distribution diagram i.e. it shifts the saturated forms formation of in the region of larger r. In the right bottom part of Fig. 2 (2d) shown F_{exp} when anti-cooperativity between sites I, II and II, III ($\boldsymbol{\omega}_1=\boldsymbol{\omega}_2=0.4$, $\boldsymbol{\omega}_3=1$) gives maximum at $r=0.57$ (formal stoichiometry is 1:1.3). At even higher anti-cooperativity we will observe the domination only complex 1:1.

4. The binding constants calculation from real experimental data

4.1. The TMPyP4 binding with tetramolecular $[d(T_4G_4)]_4$

As an example, UV-absorbance experimental data published in [12] have been used for further numerical treatment with help of proposed matrix method. When solution of $[d(T_4G_4)]_4$ added to solution of TMPyP4 in K-BPES buffer at 25 °C the induced bathochromic redshifts (422→434 nm) and hypochromicities for the Soret band are clearly indicate the DNA–ligand complexation. The cooperativity in the successive binding of TMPyP4 to the DNA in aqueous solutions was the subject of investigation. Matrix method has been used to test the hypothesis about binding stoichiometry, and to calculate parameters of TMPyP4 to DNA binding.

Fig. 3 shows function $F_{exp}=f(r)$ retrieved according to the experimental data. As can be seen from Fig. 3 the function F_{exp} have max at $r=0.7$. This result is ambiguous because value $r=0.7$ does not directly indicate definite stoichiometry of ligand with DNA interaction (for 1:2 or 1:3 theoretical value of r should be 0.67 or 0.75). First, the model taking into account the existence of 2 types of binding sites has been tested. A calculation shows that in this case the *lof* 13.9% is higher than ordinary experimental noise. Considering the existence of tree independent binding sites and non-interacting ligands ($\boldsymbol{\omega}_1=\boldsymbol{\omega}_2=\boldsymbol{\omega}_3=1$), the LS fitting in the space of 3 independent variables ($\lg \boldsymbol{K}_1=x(1)$; $\lg \boldsymbol{K}_2=x(2)$; $\lg \boldsymbol{K}_3=x(3)$) gave equal values of binding constants (see Table 2). But, the better fit to experimental curve gave theoretical function F_{calc} including the cooperativity parameter. Parameters of the best fit are given in Table 1. From this solution it is clear that the binding is positively cooperative i.e. the occupation of one binding site favors ligand association in the others.

As can be seen from Fig. 3, the theoretical dependence $F_{calc}=f(r)$ calculated according to Eq. (2) is in good agreement with the experimental data. The discrepancy between experiment and calculations is within acceptable limit of the experimental accuracy. The solution equilibrium between $[d(T_4G_4)]_4$ quadruplex (G4) and TMPyP4 (L) may be defined by equations:

$$G4 + L = G4(L) \tag{13}$$

$$G4(L) + L = G4(L)_2 \tag{14}$$

$$G4(L)_2 + L = G4(L)_3 \tag{15}$$

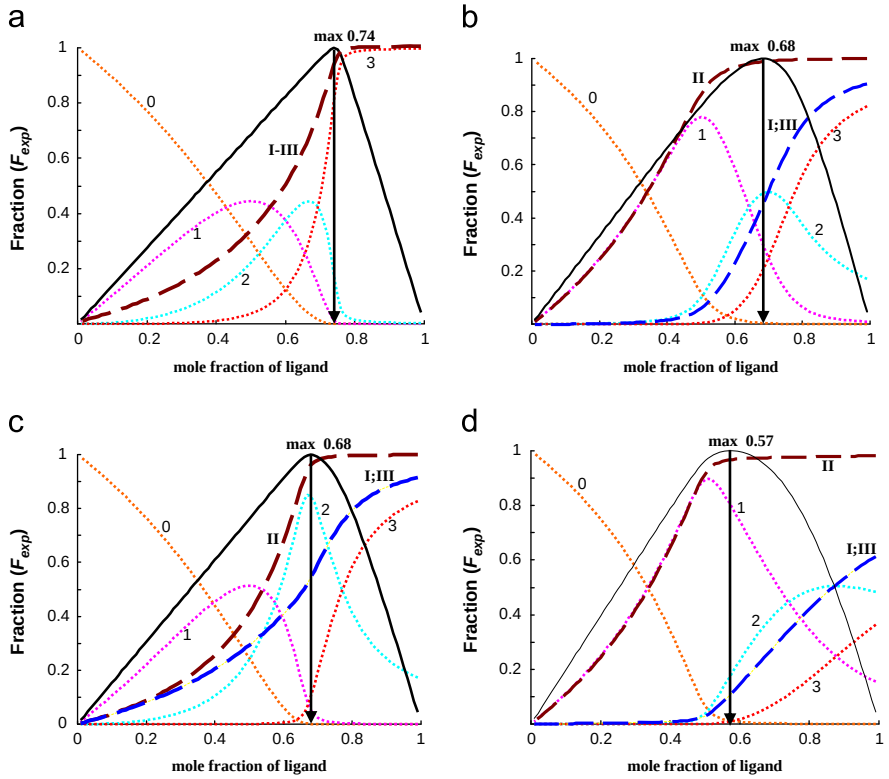

Fig. 2. Simulated Job plots (F_{exp} r.u.) for various ligands toward oligomer binding affinities shown as solid lines; (a) lg $\boldsymbol{K}_{1-3}$=**[8 8 8]**; $\omega_1=\omega_2=\omega_3=1$; (b) lg $\boldsymbol{K}_{1-3}$=**[6 8 6]**; $\omega_1=\omega_2=\omega_3=1$; and anticooperativity; (c) lg $\boldsymbol{K}_{1-3}$=**[8 8 8]**; $\omega_1=\omega_2=1$; $\omega_3=0.1$; (d) lg $\boldsymbol{K}_{1-3}$=**[6 8 6]**; $\omega_1=\omega_2=0.4$; $\omega_3=1$. The distribution plots of Poly between species [Poly](L)$_n$ as a function of ligand mole fraction (calculated by Eq. (8)) shown as dotted lines 0 – not bonded, 1 – 1:1, 2 – 1:2, 3 – 1:3; fractions of sites (I–III) bound with ligand (calculated by Eq. (9)) shown as dashed lines; $C_L+C_P=10$ μM.

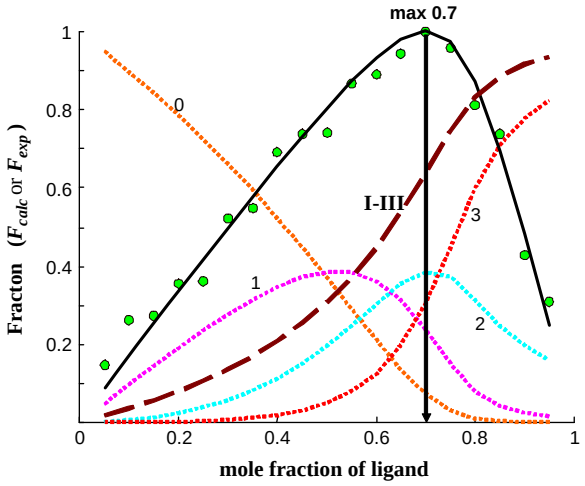

Fig. 3. Experimental and simulated Job plots for system TMPyP4-[d(T$_4$G$_4$)]$_4$. Data were reproduced from Ref. [12]. The solid line F_{calc} (r.u.) calculated as best fit to the experimental data obtained by numerical simulations based on proposed hard model lg $\boldsymbol{K}_{1-3}$=[6.25 6.25 6.25], $\boldsymbol{\omega_1=\omega_2=\omega_3=1.25}$. The filled green circles represent experimental Job plot F_{exp}(r.u.). The distribution plots of [d(T$_4$G$_4$)]$_4$ between species [d(T$_4$G$_4$)]$_4$(TMPyP4)$_n$ as a function of ligand mole fraction, calculated with the help of the matrix method shown as dotted lines 0 – not bonded, 1 – 1:1, 2 – 1:2, 3 – 1:3; fractions of sites (I–III) bound with ligand shown as dashed line; $C_L+C_P=5$ μM.; K-BPES buffer, 25 °C. (For interpretation of the references to color in this figure legend, the reader is referred to the web version of this article.)

The plot of ligand distribution between species 1:1, 1:2, 1:3 calculated from the binding constants with use of matrix method also depicted on Fig. 3. As can be seen, for the most part of the bound ligand is evenly distributed between the equilibrium complexes formed in equilibrium reactions (13)–(15). Fig. 3 plots the fraction of

Table 2
Parameters for TMPyP4 binding to G4 DNA tetraplexes obtained from Job plots.

G4 tetraplex	Number of sites	Intrinsic constants, lg $\boldsymbol{K}_{1-3}$	Cooperativity parameters, $\boldsymbol{\omega_i}$	*lof*, %
[d(T$_4$G$_4$)]$_4$	3	[6.55 6.55 6.55]	$\boldsymbol{\omega_1=\omega_2=\omega_3=1}$[a]	6.81
[d(T$_4$G$_4$)]$_4$	3	[6.25 6.25 6.25]	$\boldsymbol{\omega_1=\omega_2=\omega_3=1.25}$	6.73
[AG$_3$(T$_2$AG$_3$)$_3$]	3	[5.4 7.4 5.4]	$\boldsymbol{\omega_1=\omega_2=\omega_3=1}$[a]	1.69
[AG$_3$(T$_2$AG$_3$)$_3$]	3	[5.54 7.42 5.54]	$\boldsymbol{\omega_1=\omega_2=1}$[a], $\boldsymbol{\omega_3=0.79}$	1.36

[a] Parameters are fixed.

ligand-occupied sites versus *r*. It is worth to note that ligand-occupied sites are still equivalent. To explain the observed behavior, a non-specific electrostatic attachment of ligand to the DNA molecule is seems most evident. The phenomena of positive cooperativity probably originates from a conformational change in the DNA molecule which can lead to an energy gain when joining next ligand. It appears that shed light on a conformational change in the G4–DNA will help further investigations with help of UV-absorbance and CD spectroscopes in the region of π–π transitions in nucleic bases.

4.2. The TMPyP4 binding with intramolecular antiparallel–parallel hybrid structure [d(AG$_3$(T$_2$AG$_3$)$_3$)]

UV-absorbance experimental data published in [20] was selected to see whether proposed approach can be applied to another well characterized system. The interaction of TMPyP4 with human telomeric [d(AG$_3$(T$_2$AG$_3$)$_3$)] G-quadruplex DNA (see Scheme 3) in 150 mM K$^+$-containing buffer has been re-examined. First was tested the trial model of 1:2 binding without cooperativity. A performed calculation shows that in this case the *lof* 4.3%. The test of the trial model 1:3

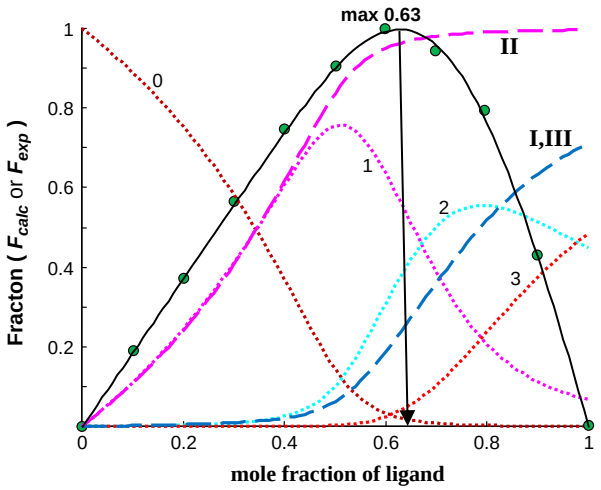

Fig. 4. Experimental and simulated Job plots for system TMPyP4-$[AG_3(T_2AG_3)_3]$. Data were reproduced from Ref. [20]. The solid line F_{calc} (r.u.) calculated as best fit to the experimental data obtained by numerical simulations based on proposed hard model $\lg \boldsymbol{K}_{1-3}$=[5.54 7.42 5.54], $\boldsymbol{\omega}_1=\boldsymbol{\omega}_2=1$, $\boldsymbol{\omega}_3=0.79$. The filled green circles represent experimental Job plot F_{exp}(r.u.). The distribution plots of $[AG_3(T_2AG_3)_3]$ between species $[AG_3(T_2AG_3)_3](TMPyP4)_n$ as a function of ligand mole fraction, calculated with the help of the matrix method shown as dotted lines 0 – not bonded, 1 – 1:1, 2 – 1:2, 3 – 1:3; fractions of sites (I–III) bound with ligand shown as dashed line; $C_L+C_P=10$ μM.; 150 mM K^+-containing buffer, 25 °C. (For interpretation of the references to color in this figure legend, the reader is referred to the web version of this article.)

binding without cooperativity gives better fit within reasonable experimental noise (*lof* 1.69%, see Table 2). However, solution still can be improved by the including of the cooperativity parameter. Parameters of the best fit are given in Table 2. Fig. 4 shows titration curve $F_{exp}=f(r)$ reconstructed according to the experimental data [20] (normalized in accordance with Eq. 1), and the fitted curve calculated with help of Eq. (2). Theoretical and experimental curves were well matched (*lof* 1.36%). The results of this analysis confirm the non-equivalence of sites which were discussed in [20], but show that a more accurate description gives the model taking into account the anti-cooperativity. The difference in the intrinsic binding constants can been attributed to steric hindrance effects, which are present in the particular G4 conformation.

The stepwise binding of the TMPyP4 ligand by $[AG_3(T_2AG_3)_3]$ quadruplex also can be written by reactions (13)–(15). Fig. 4 plots ligand distribution between successive complex species 1:1, 1:2, 1:3 calculated from the binding constants by using Eq. (8). From Fig. 4 one can conclude that a phenomenological stoichiometry 1:1.7 due to the fact that detectible formation of complex 1:3 observed only at very high ligand mole fraction. A possible explanation of the anti-cooperativity is that TMPyP4 coordinated to a free quadruplex site diminishes another site binding affinity. Besides a mutual influence between sites, an electrostatic repulsion between adjacent TMPyP4 bound ions should play important role in appearance of the anti-cooperativity.

In summary, regarding the agreement between the calculated by proposed approach and experimental data, the results suggest that those types of calculation can be used in interpretation of absorbance titration data for equilibrium systems including oligomers with different types of binding sites. The cooperativity in the successive binding of TMPyP4 to the tetramolecular $[d(T_4G_4)]_4$ and TMPyP4 anti-cooperative binding with intramolecular antiparallel–parallel hybrid structure $[AG_3(T_2AG_3)_3]$ in aqueous solutions has been discovered for the first time. This result provides new insight into the mechanism of binding between TMPyP4 and G4 DNA.

Appendix A. Supplementary materials

Supplementary data associated with this article can be found in the online version at http://dx.doi.org/10.1016/j.talanta.2013.07.012.

References

[1] S. Neidle, S. Balasubramanian, Quadruplex Nucleic Acids, The Royal Society of Chemistry, Cambridge, 2006.
[2] P. Murat, Y. Singh, E. Defrancq, Chem. Soc. Rev. 40 (2011) 5293.
[3] F.X. Han, R.T. Wheelhouse, L.H. Hurley, J. Am. Chem. Soc. 121 (1999) 3561.
[4] M.Y. Kim, M. Gleason-Guzman, E. Izbicka, D. Nishioka, L.H. Hurley, Cancer Res. 63 (2003) 3247.
[5] N.V. Anantha, M. Azam, R.D. Sheardy, Biochemistry 37 (1998) 2709.
[6] S.N. Georgiades, N.H. Abd Karim, K. Suntharalingam, R. Vilar, Angew. Chem. Int. Ed. 49 (2010) 4020.
[7] R.T. Wheelhouse, D. Sun, H. Han, F.X. Han, L.H. Hurley, J. Am. Chem. Soc. 120 (1998) 3261.
[8] L. Martino, B. Pagano, I. Fotticchia, S. Neidle, C. Giancola, J. Phys. Chem. B 113 (2009) 14779.
[9] H.J. Zhang, X.F. Wang, P. Wang, X.C. Ai, J.P. Zhang, Photochem. Photobiol. Sci. 7 (2008) 948.
[10] Stephen Neidle, Curr. Opin. Struct. Biol. 19 (2009) 239.
[11] M.J. Morris, K.L. Wingate, J. Silwal, T.C. Leeper, S. Basu, Nucleic Acids Res. 40 (2012) 4137.
[12] I. Haq, J.O. Trent, B.Z. Chowdhry, T.C. Jenkins, J. Am. Chem. Soc. 121 (1999) 1768.
[13] H. Han, D.R. Langley, A. Rangan, L.H. Hurley, J. Am. Chem. Soc. 123 (2001) 8902.
[14] C. Wei, G. Jia, J. Yuan, Z. Feng, C. Li, Biochemistry 45 (2006) 6681.
[15] G.N. Parkinson, R. Ghosh, S. Neidle, Biochemistry 46 (2007) 2390.
[16] I. Lubitz, N. Borovok, A. Kotlyar, Biochemistry 46 (2007) 12925.
[17] S. Cogoi, M. Paramasivam, B. Spolaore, L.E. Xodo, Nucleic Acids Res. 36 (2008) 3765.
[18] S. Cogoi, L.E. Xodo, Nucleic Acids Res. 34 (2006) 2536.
[19] G. Jia, Z. Feng, C. Wei, J. Zhou, X. Wang, C. Li, J. Phys. Chem. B 113 (2009) 16237.
[20] C. Wei, G. Jia, J. Zhou, G. Han, C. Li, Phys. Chem. Chem. Phys. 11 (2009) 4025.
[21] A. Arora, S. Maiti, J. Phys. Chem. B 112 (2008) 8151.
[22] A. Arora, S. Maiti, J. Phys. Chem. B 113 (2009) 8784.
[23] J. Jaumot, R. Eritja, R. Gargallo, Anal. Bioanal. Chem. 399 (2011) 1983.
[24] S. Manaye, R. Eritja, A. Avino, J. Jaumot, R. Gargallo, Biochim. Biophys. Acta 1820 (2012) 1987.
[25] M.W. Freyer, R. Buscaglia, K. Kaplan, D. Cashman, L.H. Hurley, E.A. Lewis, Biophys. J. 92 (2007) 2007.
[26] J.B. Chaires, Methods Enzymol. 340 (2001) 3.
[27] N. Hadjiliadis, E. Sletten, Metal Complex–DNA Interactions, Blackwell Publishing Ltd., Oxford, 2009.
[28] H. Yaku, T. Murashima, T. Miyoshi, N. Sugimoto, Molecules 17 (2012) 10586.
[29] T.L. Hill, Cooperativity Theory in Biochemistry. Steady State and Equilibrium Systems, Springer Verlag, New York, 1985.
[30] D.M. Crothers, Biopolymers 6 (1968) 575–584.
[31] G. Schwarz, Eur. J. Biochem. 12 (1970) 442–453.
[32] E. Cera, Thermodynamic Theory of Site-Specific Binding Processes in Biological Macromolecules, Cambridge University Press, Cambridge, 1995.
[33] Yu.D. Nechipurenko, G.V. Gursky, Biophysics 48 (2003) 717–740.
[34] J.L. Garcés, C. Rey-Castro, C. David, S. Madurga, F. Mas, I. Pastor, J. Puy, J. Phys. Chem. B 113 (2009) 15145.
[35] J.D. McGhee, P.H. von Hippel, J. Mol. Biol. 86 (1974) 469.
[36] G. Scatchard, N.Y. Ann, Acad. Sci 51 (1949) 660.
[37] A.G. Kudrev, Talanta 101 (2012) 157.
[38] A.G. Kudrev, Talanta 75 (2008) 380.
[39] A.Yu. Timoshkin, A.G. Kudrev, Russ. J. Inorg. Chem. 57 (2012) 1362.
[40] A.G. Kudrev, Polym. Sci. Ser. A 42 (2000) 527.
[41] A.G. Kudrev, Russ. J. Gen. Chem. 72 (2002) 1501.
[42] A.G. Kudrev, Russ. J. Gen. Chem. 11 (2006) 1782.
[43] R. Gargallo, R. Eritja, A.G. Kudrev, Russ. J. Gen. Chem. 80 (2010) 485.
[44] P. Bucek, R. Gargallo, A. Kudrev, Anal. Chim. Acta 683 (2010) 69.
[45] A.G. Kudrev, Biophysics 57 (2012) 305.
[46] D.W. Marquardt, J. Soc. Ind. Appl. Math. 2 (1963) 431.
[47] M. Maeder, A.D. Zuberbühler, Anal. Chem. 62 (1990) 2220.
[48] R.M. Dyson, S. Kaderli, G.A. Lawrance, M. Maeder, A. D. Zuberbühler, Anal. Chim. Acta 353 (1997) 381.
[49] W.C. Hamilton, Statistics in Physical Science, Roland Press, NY, 1964.